# *Chapter-IV*

## Magnetic Properties

# Chapter IV

# MAGNETIC PROPERTIES

## PART A

## MAGNETIC HYSTERESIS

### 4.A.1 Introduction

Magnetic properties of ferrites are as important as their electrical properties. The choice of a ferrite for a particular application is decided by its data on saturation magnetization, coercive force, remanence ratio, permeability susceptibility etc. With the help of hysteresis studies one can determine magnetization, coercive force and remanence ratio. The ferrites with low coercive force (Hc) are called as "soft ferrites". Generally they have high electrical resistivity and hence low eddy current losses. These ferrites are widely used in microwave devices, high frequency cores, antennas, transformer etc. The ferrites with high coercive force (Hc) are called as "hard ferrites". These ferrites are used in electric motors, generators, loud speakers and television sets as permanent magnets.

Ferrites with square loop are widely used as computer memory devices. The coercive force varies from 0.1 to 3 kOe depending on

porosity, anisotropy, saturation magnetization etc. [1]. The origin of magnetization is in the alignment interactions which arise of magnetic dipoles to form an internal magnetic field called "Weiss Molecular field" [2]. However quantum mechanics relates this to the "exchange interaction" [3].

The slope of hysteresis loop ($\mu$) is a structure sensitive property. These properties are also influenced by the sintering condition, sintering atmosphere and the rate of cooing etc. The porosity, grain size and stoichiometry have been especially important in controlling the magnetic properties of ferrites.

### 4.A.2 Magnetization

Spontaneous magnetization is characteristic of ferrimagnetic materials. Spontaneous magnetization arises if the magnetic atoms are sufficiently close to each other. The electrons can undergo on exchange between neighbouring magnetic atoms. The exchange interaction between neighbouring atoms may be direct or may take place via intermediate non-magnetic ions such as oxygen [4]. The coupling between magnetic atoms in a substance may be parallel or anti-parallel alignment of the spins of the neighbouring atoms. When the alignment is parallel, ferromagnetism results and when it is anti-parallel anti-ferromagnetism or ferrimagnetism results.

Ferrite is the ferrimagnetic material containing two sets of moments A and B. All the A moments are aligned and so also the B moments. The resulting magnetic moment arises from the anti parallel alignments of A moments with B moments. Neel [5] developed the theory of magnetization. The normal spinels are non-magnetic while inverse spinels are ferrimagnetic.

The interaction between the spins can be explained quantum mechanically as,

$$E = -2\ Je\ \vec{Si}.\ \vec{Sj} = -2\ Je\ Si\ Sj\ \cos\theta \qquad \text{----4.1}$$

where Je - Exchange Integral

$\vec{Si}$ = Spin on $i^{th}$ atom due to electrons.

$\vec{Sj}$ = Spin on $j^{th}$ atom due to electrons.

$\theta$ = Angle between spins Si and Sj

Je measures the extents to which the electronic change distribution of two atoms overlaps one another. The electrons under consideration spend a fraction of their time around the nuclei of both the atoms. For non violation of Pauli's exclusion principle, electrons must be exchanged between the atoms. The direct exchange may be either positive or negative.

Three kinds of magnetic interactions between the ions situated on A and B sites, viz A-A, B-B and A-B interactions occur in ferrites [6].

Fig.4.A.1. The A-B interaction is of greatest magnitude. The two configurations for A-B interaction have small distance and the values of the angle $\phi$ are fairly high. The A-A interaction is weakest interaction as the distance 'r' is large and the angle $\phi$ is 180°. The angle of $\phi$ = 180° gives rise to the greatest exchange energy and the energy decreases very rapidly with increasing distance. For perfect spinel lattice the major angles between the ions are ABO (125°9' and 154° 34'), BOB (90° and 125°9') and AOA (79° 38').

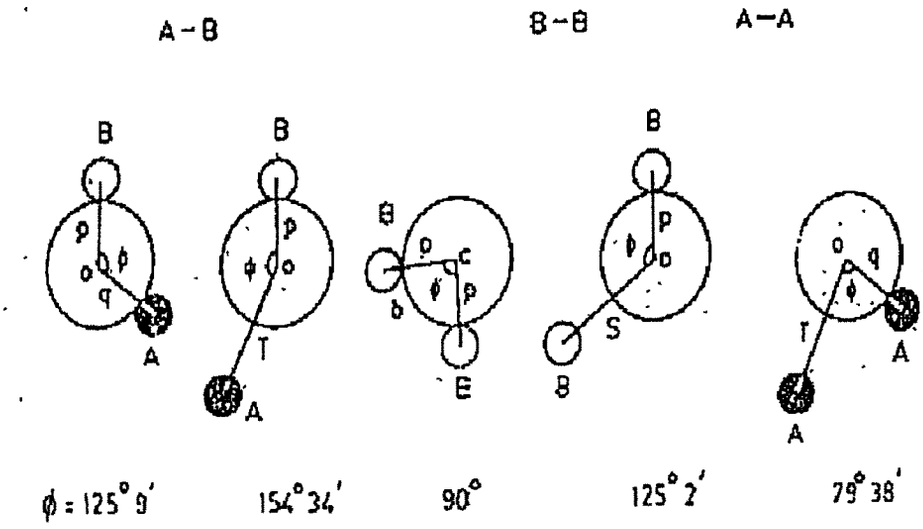


**Fig. 4.A.1 - Possible configurations of ion pairs in spinel ferrites**

### 4.A.3 Magnetic hysteresis

When a ferromagnetic substance in subjected to an external magnetic field, the domains start orienting in the direction of the applied field. Hysteresis is the phenomenon in which magnetic induction lags behind the applied magnetic field. As the magnetic field is increased further, there is irreversible boundary displacement and at first induced magnetization increases rapidly than the field strength. All the boundaries get displaced and further increase in magnetic field causes rotation of domains in the direction of applied magnetic field. The material is said to be saturated magnetized. After the magnetic field is decreased to zero, the alignment of most of the domains remains unchanged and gives raise the remanent magnetization ($M_r$). When the direction of applied magnetic field is reversed, at the certain value of magnetic field the remanent magnetization becomes zero. It is called as "coercivity (Hc). The variation of magnetization over one complete cycle of external magnetizing field is called hysteresis loop (Fig. 4.A.2).

Hysteresis study on ferrites provides valuable information on permeability, saturation magnetization, coercive force and remanence ratio. From the B-H curve, the slope of tangent at the origin gives the initial permeability ($\mu_i$). The maximum permeability occurs at the knee of the magnetization curve. These hysteresis properties are helpful in deciding the nature of application of ferrites. The hysteresis properties

mainly depends on the chemical composition, crystal structure, cation distribution and microstructure [7, 8]

The ferrimagnetic or ferromagnetic material is divided into small regions called domains, suggested by Weiss [2]. The Weiss domains in the absence of the external magnetic field are randomly oriented resulting in zero magnetization. Moreover these domains are separated by a thin layer in which the direction of the magnetization changes from one orientation to another. Bean [9] on the basis of hysteresis phenomenon has classified the magnetic particles in to 'single domain' (SD), 'multidomain' (MD), 'superparamagnetic' (SP).

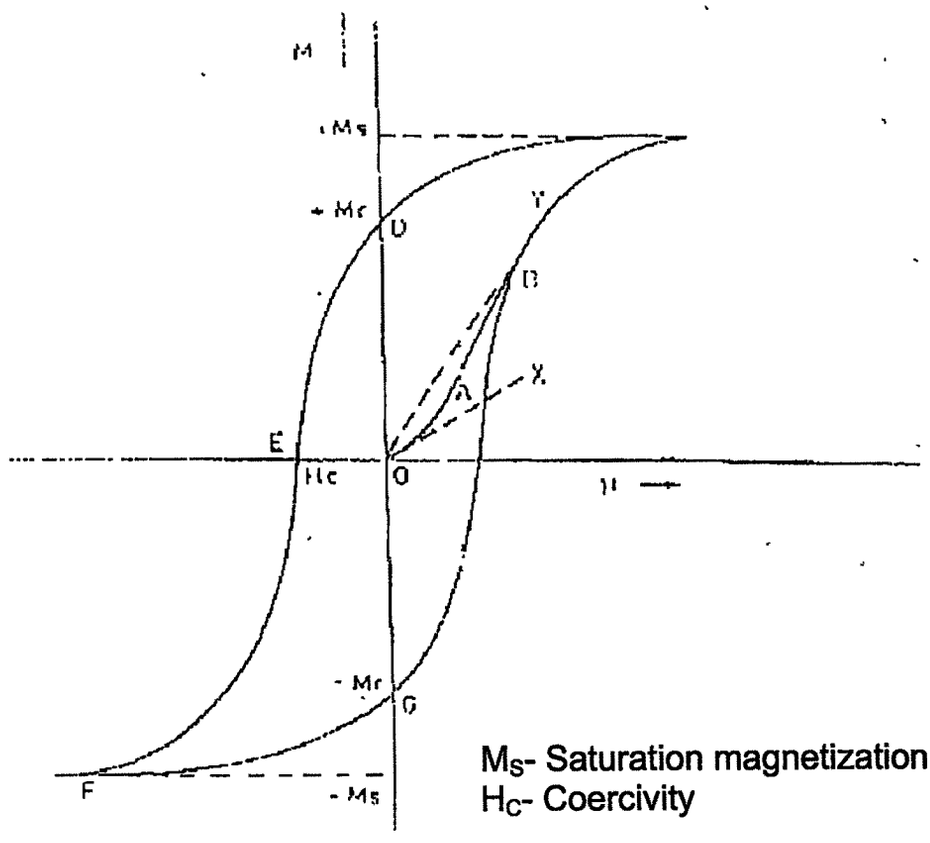


Fig. 4.A.2 - Magnetic Hysteresis Curve

### 4.A.4 Experimental technique

High field hysteresis loop tracer designed by Tata Institute of Fundamental Research, Bombay was used to measure the magnetization of the samples.

The apparatus is set up by using a standard nickel sample whose saturation magnetization per unit mass is known and calibration factor (CF) is automatically recorded. the values of saturation magnetization ($M_s$), remanence magnetization and coercive force are directly recorded by the computer.

### 4.A.5 Results and discussion

The hysteresis loops for the samples in the series $Li_{0.5}Ni_{1.5x}Fe_{2.5-x}O_4$ ferrites (where x = 0.1, 0.2, 0.3, 0.4 and 0.5) are shown in Fig. 4.A.3 to 4.A.7. The values of saturation magnetization (Ms) and Magnetic moment ($\eta_B$) calculated from the hysteresis data are given in Table 4.1.

From this, it can be observed that the magnetic moment $\eta_B$ and saturation magnetization increase and have maximum values at x = 0.2. They decrease with further Ni content [16]. The magnetization in ferrites results from the distribution and alignment of magnetic ions on tetrahedral and octahedral sites. Nickel ferrite cooled slowly from sintering temperature has a structure of a complete inverse spinel.

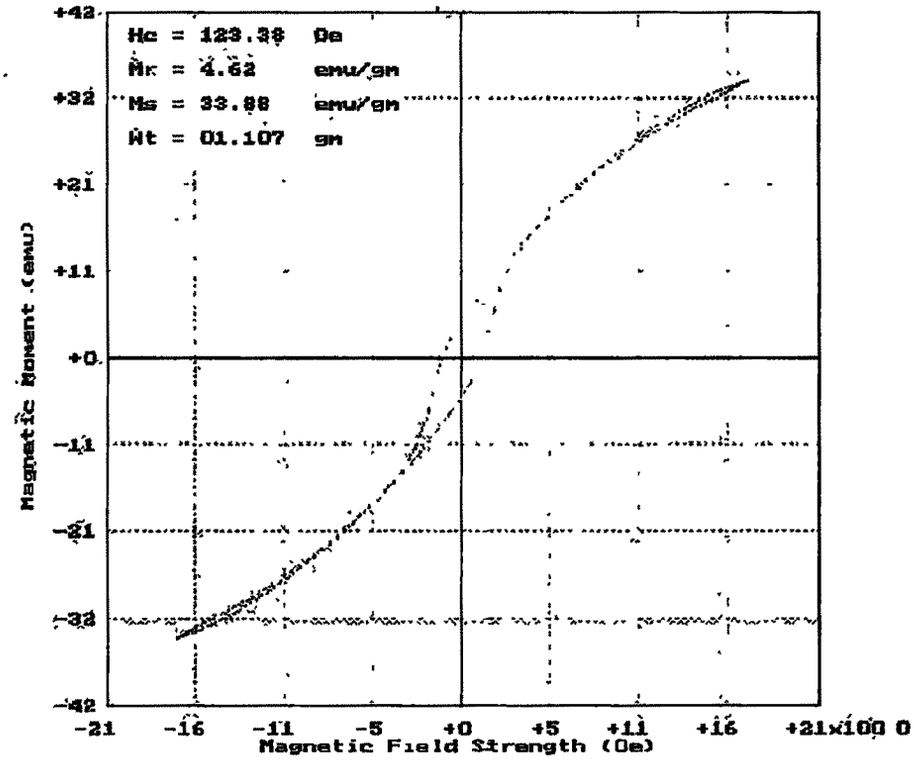


Fig. 4.A.3 – Hysteresis loop for $Li_{0.5}Ni_{0.15}Fe_{2.4}O_4$ ferrite.

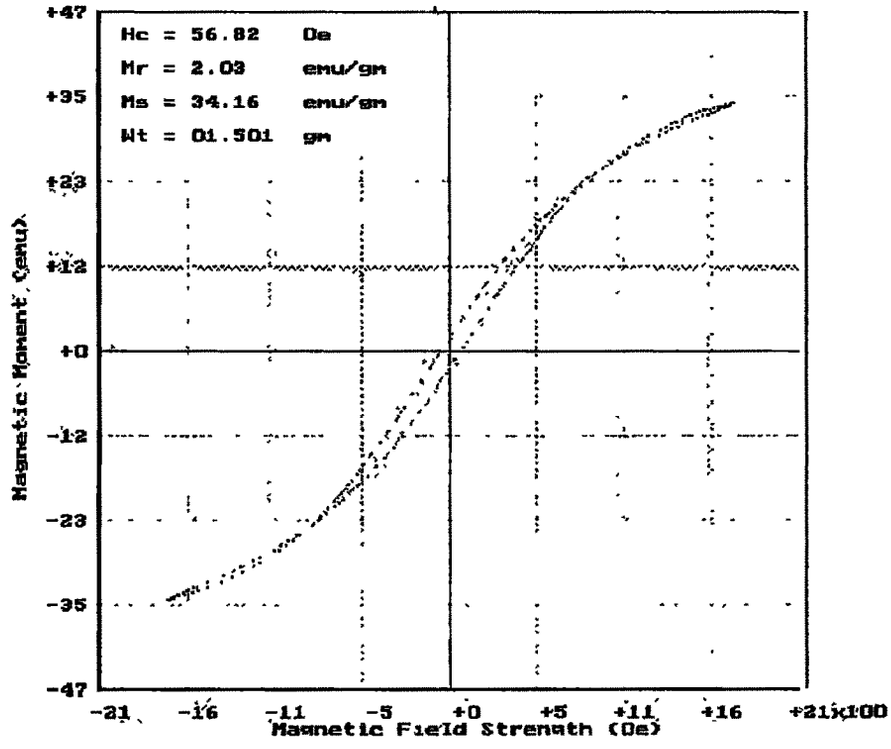


Fig. 4.A.4 – Hysteresis loop for $Li_{0.5}Ni_{0.3}Fe_{2.3}O_4$ ferrite.

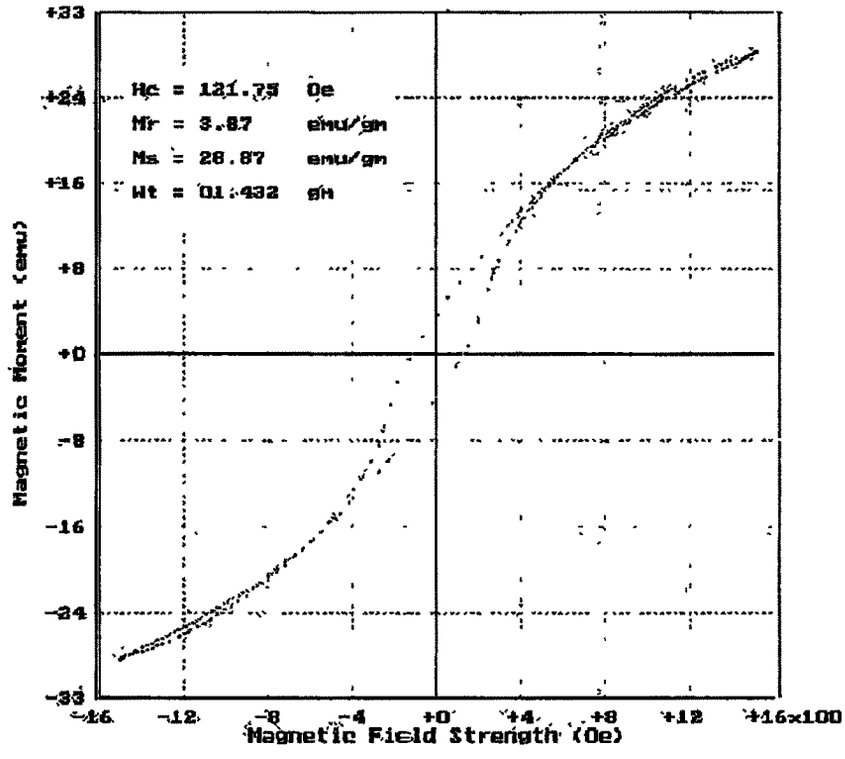


Fig. 4.A.5 – Hysteresis loop for $Li_{0.5}Ni_{0.45}Fe_{2.2}O_4$ ferrite.

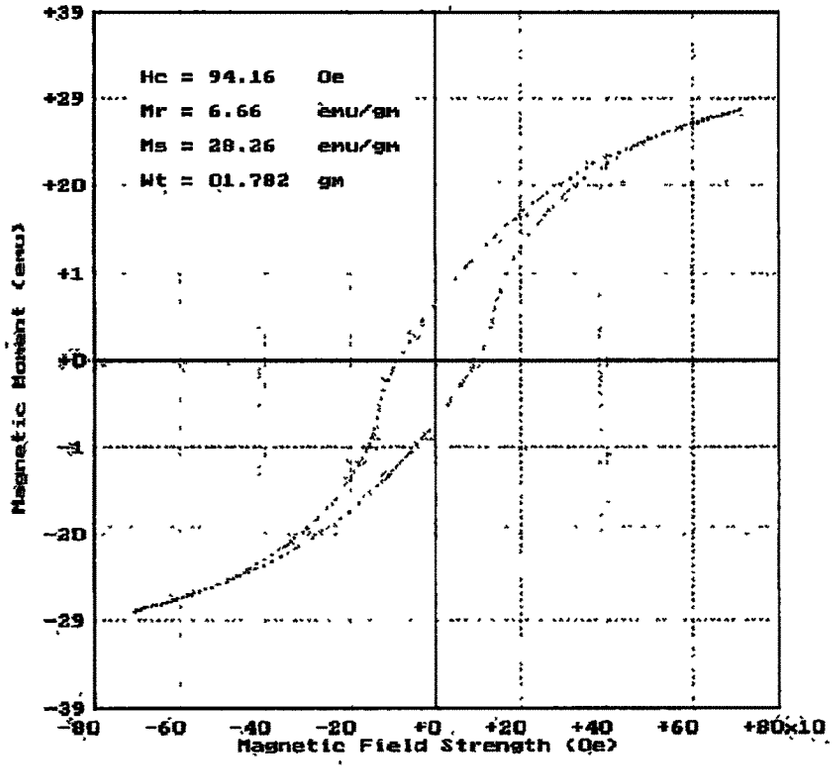


Fig. 4.A.6 – Hysteresis loop for $Li_{0.5}Ni_{0.6}Fe_{2.1}O_4$ ferrite.

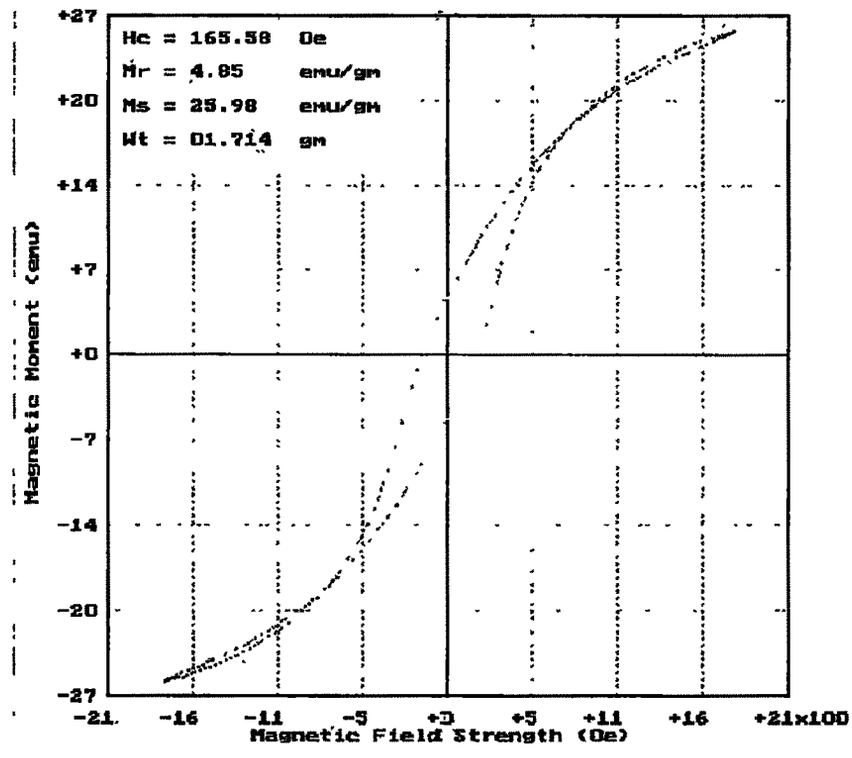


Fig. 4.A.7 – Hysteresis loop for $Li_{0.5}Ni_{0.75}Fe_2O_4$ ferrite.

**Table 4.1** Data on saturation magnetization (Ms) and magnetic moment ($\eta_B$) for $Li_{0.5}Ni_{1\pm x}Fe_{2.5-x}O_4$ ferrites.

| Sample 'x' | Magnetic Moment $\eta_B$ | Ms emu / gm. | $4\pi M_S$ emu / gm |
|---|---|---|---|
| 0.1 | 1.319 | 33.88 | 425.87 |
| 0.2 | 1.348 | 34.16 | 429.39 |
| 0.3 | 1.219 | 30.50 | 383.39 |
| 0.4 | 1.145 | 28.21 | 355.23 |
| 0.5 | 1.125 | 27.43 | 344.80 |

On the basis of preference of the ions and saturation magnetization the cation distribution for the present system can be proposed as

$$\left[Fe^{3+}_{1.25-0.66x}Ni^{2+}_{0.75x}\right]^{A}\left[Li^{1+}_{0.5}Ni^{2+}_{0.75x}Fe^{3+}_{1.25+0.66x}\right]^{B}O^{2-}_{4}$$

The magnetic moment for $Ni^{2+}$ is 2.2 $\mu_B$ and for $Fe^{3+}$ it is 5$\mu_B$ [10]. The $Fe^{3+}$ ions on A sites are coupled with their spin antiparallel to the $Fe^{3+}$ ions on B-sites. So that the net magnetic moment is due to $Ni^{2+}$ ions. The variation of magnetic moment ($\eta_B$) and saturation magnetization ($M_S$) with Ni content is shown in Fig. 4.A.8 and 4.B.9.

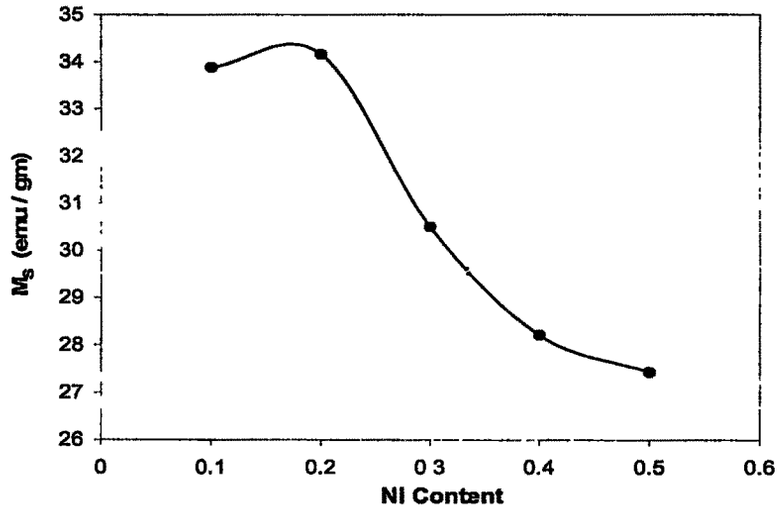


**Fig.4.A.7 Variation of satuaration magnetization with NI Content for $Li_{0.5}NI_{1.5x}Fe_{2.5-x}O_4$ ferrites**

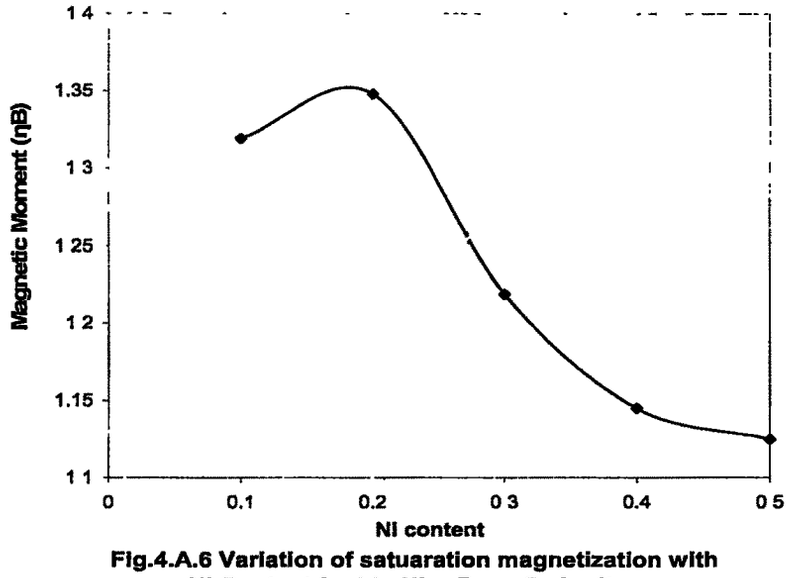


**Fig.4.A.6 Variation of satuaration magnetization with Ni Content for $Li_{0.5}NI_{1\ 5x}Fe_{2.5-x}O_4$ ferrites**

The variation of Ms and $\eta_B$ in the present case can be explained as follows: The substitution of $Ni^{2+}$ ions at B-site transfers $Fe^{3+}$ ions from B-site to A-site and affects the magnetic moment of an individual sublattices as well as the A-B interaction. This results in the increase of saturation magnetization. Further $Ni^{2+}$ substitution in lithium ferrite weakens the A-B interaction and prefers the B-B interaction and hence the net magnetic moment decreases. This results in the increase of Ms and $\eta_B$ for the composition with x = 0.2. The decrease in saturation magnetization in the samples can be explained on the basis of the change in the magnetization $M_A$ and $M_B$ on tetrahedral and octahedral sub lattices respectively. The partial replacement of $Fe^{3+}$ions by $Ni^{2+}$ions results in lowering of values of $M_A$ and $M_B$. The decrease of $[M_A-M_B]$ there by decreases the net magnetization and hence the magnetic moment.

In the present nanocrystalline lithium nickel ferrites, the saturation magnetization (Ms) is found to be lower than that of bulk nickel ferrite because of their small gain size. Also the saturation magnetization depends on the surface roughness at room temperature as reported by Nathani [11]. He has reported that the hysteresis loop of nanocrystalline nickel ferrite becomes non-squared and the coercivity increases with increase in surface roughness. Similar result is reported by Parker [12].

The origin of surface spin disorder for nickel ferrite nanoparticles may be due to broken exchange bonds, high anisotropy layer on the

surface, or a loss of the long-range order in the surface layer. These effects are particular strong in the case of ferrites because of the super-exchange interactions through the oxygen ions. If often happens that two magnetic ions are separated by nonmagnetic ion. Y Cheng et al. [13] have reported low coercivity and high saturation magnetization, which is probably due to their unique face octahedral morphology. The magnetic behaviour of nanoparticles has a marked dependence on decrease in particle size and the surface effects start to dominate [15, 16]. Nathani [17] has reported jump in the initial part of the magnetization curve, which implies the existence of a core shell like morphology of the particles of nanocrystalline nickel ferrite.

# PART B
# A.C. SUSCEPTIBILITY

## 4.B.1 Introduction

A. C. susceptibility studies explore the existence of single domain (SD), multidomain (MD) and superparamagnetic (SP) particles in the material. The large grains with domain size ranging from 1 x $10^{-6}$ to $10^{-5}$ cm are called multi-domain. The small magnetic particles without domain walls are called single domain (SD) particles. The particle of size smaller than 6 x $10^{-8}$ cm are called superparamagnetic (SP) particle. The change of a. c. susceptibility in ferrite with temperature is correlated with domain structure [18]. The Curie temperature of ferrites has been reported by many workers from $\chi_{ac}$-T plots [19, 20]. The coercive force for single domain is very large and for supermagnetic particle it becomes zero, as reported by Bean [9].

The variation of a. c. susceptibility with temperature for ferrimagnetic iron shows that it reaches a peak value just before Curie temperature and becomes rapidly zero at $T_c$ [21]. It is also reported that the peaks in $\chi_{ac}$ -T curves depend on the size of the magnetic particles.

When the thermal energy of SP particles becomes comparable to effective magnetic anisotropy energy, magnetization direction fluctuates

about the easy axis of the grain. In such a state, the grain is said to be exhibiting super-paramagnetism and for the volume V of the grain, the temperature is referred to as blocking temperature ($T_b$), which will be less than the Curie temperature (Tc) of the concerned material. The volume V and the saturation magnetization Ms are related by equation

$$V\ Ms\ Hc = 2kT_b \qquad \text{---- 4.2}$$

where k is Boltzmann constant. Thus SP can be changed to SD by cooling the ferrites below their $T_b$.

**4.B.2 Experimental**

The variation of normalized a. c. susceptibility of the present samples as a function of temperature was measured with the help of experimental setup developed by Tata Institute of Fundamental Research, Bombay. The apparatus consists of double coil set up. One coil produces a 7 $O_e$ magnetic field at 263 Hz and another coil produce a emf directly proportional to the susceptibility of the sample.

**4.B.3 Results and discussion**

The variation of normalized a. c. susceptibility of the present $Li_{0.5}Ni_{1.5x}Fe_{2.5-x}O_4$ (x = 0.1, 0.2, 0.3, 0.4 and 0.5) ferrite samples as a function of temperature is shown in Fig. 4.B.1. From the figure it is observed that,

1. The normalized a. c. susceptibility does not appreciably change with temperature and sharply drop off at the Curie temperature,

for x = 0.4 and 0.5 indicating MD particles in the samples. However for x = 0.1, 0.2 and 0.3 normalized ac susceptibility decreases with temperature indicating SP particles.

2. The sharp fall at 'Tc', shows the single phase formation of ferrites with no impurities.
3. Curie temperature increases on the addition of nickel.
4. It is concluded that the ferrite samples with x = 0.1, 0.2, 0.3 0.4 and 0.5 contains MD as well as SP particles.

Naik et al. [22] have studied a. c. susceptibility of Li-Cu ferrites. They have reported a decrease in peaking behaviour with addition of Lithium. They have attributed the suppression to the increase in MD nature of samples. Shaikh et al [23] have studied variation of $\chi_{ac}$ -T curves of Li-Mg-Zn ferrites and reported that the samples with Zn = 0.1 to 0.5 contain multidomain (MD) particles. Bellad et al. [24] have reported the presence of multi domain (MD) particles in Li-Cd ferrites. Patil et al. [25, 26] have reported the similar results in case of Zr-Zn and Zn-Ti substituted Li-ferrites.

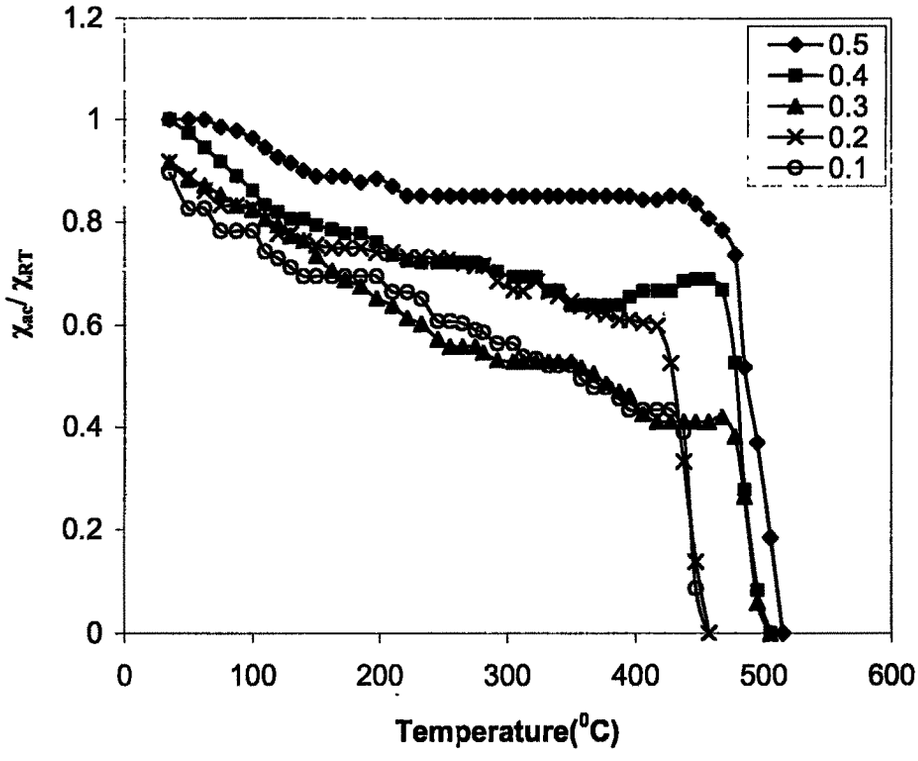


**Fig. 4.B.1 - Variation of susceptiblity with temperature for $Li_{0.5}$ $Ni_{1.5X}$ $Fe_{2.5-X}$ $O_4$ Ferrites**

**References**


1 A. M. Alper
"High Temperature Oxides"
Academic Press, New York (1971)

2 P. J. Weiss
J. Phys. Theo. Appl. 6 (1907) 677

3 W. Z. Heisenberg
J. Phys. 49 (1978) 619

4 K. Hoselists
"Magnetic properties" in "Physical Metallurgy"
North Holland Pub. Co. London (1970) 1233

5 L. Neel
Ann. Phys. (Paris) 3 (1948) 137

6 E. W. Gorter
Nature 165 (1950) 798

7 H. Igarashi and K Okazaki
J. Amer. Ceram. Soc. (USA) 50 (1977) 51

8 X. L. Sean
JEEE Trans. Mag. 22 (1986) 14

9 C. P. Bean
J. Appl. Phys. 26 (1955) 1381.

10 J. M. Robertson and A. J. Pointon
Solid State Comm. 4 (1966) 257

11 H. Nathani, S. Gubbala and R. D. K. Misra.
Mater. Sci. Engg. B 121 (2005) 126-136

12 F. T. Parker, M. W. Foster, D. T. Margules and A Berkowitz
Phys. Rev. B 7 (1990) 7885

13 Y. Cheng, Y. Zheng, Y. Wang, F. Bao and Y. Qin
J. Solid Stat. Chem. 178 (2005) 2394-2397

14 G. Caruntu, I. Dumitru, G. G. Bush, D. Caruntu and C. J O'Connor
J. Phys. D: Appl. Phys. 38 (2005) 811-815

15 M. E. McHenry and D. E. Loughin
Acta. Mater. 48 (2000) 223

16 C. Caizer and M. Stefanescu
J. Phys. D: Appl. Phys. 35 (2002) 3035-3040

17 H. Nathani and R. D. K. Misra
Mater. Sci. Engg. B 113 (2004) 228-235

18 C. R. Murthy
J. Geolog. Soc. India 26 (a) (1985) 640

19 R. G. Kulkarni and R. V. Upadhyay
Mat. Lett. 4 (3) (1986) 168

20 S. H. Patil S. I. Patil, S. M. Kadam and B. K. Chougule
Indian J. Pure Appl. Phys. 30 (1992) 183

21 J. Hopkinson
Phil. Trans. Royal Soc. (London) A 180 (1989) 443

22 B. Naik and J.I. Pawar
Indian J. Pure Appl. Phys. 23 (1985) 436

23 A. M. Shaikh, S. C. Watave, S. S. Bellad, S. A. Jadhav and B. K. Chougule
Mat. Chem. Phys. 65 (2000) 46

24 S. S. Bellad, S. C. Watave and B.K. Chougule
J. Magn. Magn. Mater. 195 (1999) 57

25 R. S. Patil
J. Magn. and Magn. Mater. 103 (1991) 51

26 R. S. Patil
J. Magn. and Magn. Mater. 25 (1991) 355